

Gapless Coulomb state emerging from a self-dual topological tensor-network state

Guo-Yi Zhu¹ and Guang-Ming Zhang^{1,2}

¹State Key Laboratory of Low-Dimensional Quantum Physics and
Department of Physics, Tsinghua University, Beijing 100084, China

²Collaborative Innovation Center of Quantum Matter, Beijing 100084, China.

(Dated: March 11, 2024)

In the tensor network representation, a deformed Z_2 topological ground state wave function is proposed and its norm can be exactly mapped to the two-dimensional solvable Ashkin-Teller (AT) model. Then the topological (toric code) phase with anyonic excitations corresponds to the partial order phase of the AT model, and possible topological phase transitions are precisely determined. With the electric-magnetic self-duality, a novel gapless Coulomb state with quasi-long-range order is obtained via a quantum Kosterlitz-Thouless phase transition. The corresponding ground state is a condensate of pairs of logarithmically confined electric charges and magnetic fluxes, and the scaling behavior of various anyon correlations can be exactly derived, revealing the effective interaction between anyons and their condensation. Deformations away from the self-duality drive the Coulomb state into either the gapped Higgs phase or confining phase.

Introduction.— The toric code model proposed by Kitaev[1] is a prototypical model realizing the Z_2 intrinsic topological phase of matter with anyonic excitations. It is interesting and fundamentally important to consider the possible topological phase transitions out of the toric code phase, because such phase transitions are beyond the conventional Ginzburg-Landau paradigm for the symmetry breaking phases. From the perspective of lattice gauge theory, it has been known that there exists the Higgs/confinement transition, where the electric charge is condensed/confined accompanied by the confinement/condensation of magnetic flux due to electric-magnetic duality[2–7]. However, there is a long-standing puzzle: what is the nature of the phase transition along the self-dual line and how the Higgs and confinement transition lines merge into the self-dual phase transition point[6, 8]. Should there be a tricritical point, it would go beyond the anyon condensation scenario[9], because the electric charge and magnetic flux are not allowed to simultaneously condense.

In this Letter, we shall resolve this puzzle and provide new insight into the nature of this topological phase transition. Instead of solving a Hamiltonian with tuning parameters, we propose a deformed topological wave-function interpolating from the nontrivial to trivial phases in the tensor network representation[10–12], which provides a clearer scope into the essential physics of abelian anyonic excitations[13–17]. In this scheme, the usual pure Higgs/confinement transition of the toric code[14, 18, 19] has a special path, where the deformed wave-function can be exactly mapped to a two-dimensional (2D) classical Ising model. The topological phase transition is associated with the 2D Ising phase transition, drawing the striking topological-symmetry-breaking correspondence[20].

Further deformation of the toric code wave functions can span a generalized phase diagram[21–23], where the perturbed Higgs and confinement transitions were gener-

ically obtained by the symmetry breaking pattern and long-range-order in the virtual space of transfer matrix in the tensor-network formalism[15, 16]. But the nature of the phase transition along the self-dual path remains elusive. By proposing a new version of the deformed topological tensor network wave function, we prove that the whole phase diagram can be exactly mapped to a 2D classical isotropic Ashkin-Teller (AT) model, and the toric code phase is associated with the partial order phase of the AT model. It is in the same spirit of the plasma analogy for fractional quantum Hall phases[24]. Such a mapping not only sheds new light on the hidden structure of the topological phase transitions, but also enables us to analytically pinpoint the accurate positions of the critical point and extract the scaling behavior of the anyon correlation functions. More importantly, we find that the toric code phase along the self-dual path undergoes a quantum Kosterlitz-Thouless (KT) transition into the gapless Coulomb state with quasi-long-range order[25], which is truly beyond the Ginzburg-Landau paradigm.

Wave-function deformation.— The toric code model on a square lattice with periodic boundary condition is

$$H_{\text{TC}} = - \sum_j A_j - \sum_p B_p, \quad (1)$$

where the star operator $A_j = \prod_{i \in \text{star}(j)} \sigma_{i,j}^x$ lives on the vertex j , and plaquette operator $B_p = \prod_{\langle i,j \rangle \in \partial p} \sigma_{i,j}^z$ lives on the plaquette p (Fig. 1a). The ground states are stabilized by $A_j = 1 \forall j$, $B_p = 1 \forall p$, and $A_j = -1$ is associated to an electric charge excitation while $B_p = -1$ to a magnetic flux excitation. The bare model is invariant under the electric-magnetic duality:

$$\mathcal{D} : \sigma^x \leftrightarrow \sigma^z, j \leftrightarrow p. \quad (2)$$

If the spin up is viewed as a reference basis and the spin down as a segment of magnetic flux tubes, the ground state is a condensate of closed magnetic loops[26], or electric loops by duality. On a torus, the four-fold ground

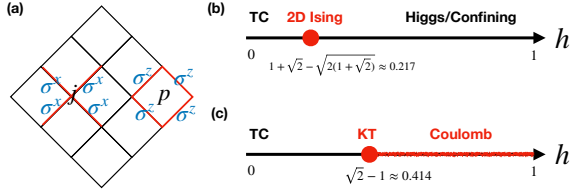


FIG. 1: (a) Bare Hamiltonian terms of the toric code model. (b) The 2D Ising conformal quantum critical point encountered by the toric code phase along the Higgs/confinement transition. (c) The 2D KT conformal quantum phase transition of the toric code phase along the electric-magnetic self-dual path.

states can be labeled by the evenness of global noncontractible electric/magnetic loops along x direction, in one-to-one correspondence with the four anyon sectors: $1, e, m, f$. The vacuum state has even number of both electric and magnetic noncontractible loops along x :

$$|1\rangle = \frac{1 + M_y}{\sqrt{2}} \prod_j (1 + A_j) |\uparrow\rangle_\sigma, \quad (3)$$

where $|\uparrow\rangle_\sigma \equiv \prod_{\langle i,j \rangle} |\uparrow\rangle_{i,j}$ is the reference state, and M_y is the dual Wilson line that pumps a magnetic flux tube wrapping around the torus in y direction. It can be checked that $|1\rangle$ is invariant under electric-magnetic duality: $\mathcal{D}|1\rangle = |1\rangle$.

In general, one can deform the toric code wave-function by filtering with the spin polarized channel[21]:

$$|\psi(h, \theta)\rangle = \prod_{\langle i,j \rangle} [1 + h (\sigma_{i,j}^z \sin\theta + \sigma_{i,j}^x \cos\theta)] |1\rangle, \quad (4)$$

where $h \in [0, 1)$ expresses the strength of filtering and $\theta \in [0, \pi/2]$ is the spin angle. The limit $h \rightarrow 1$ tends to filter out the spin polarized trivial state. When $\theta = \pi/2$, the deformed wave-function only contains closed magnetic loop configurations and has been well studied[14, 18, 19, 27]. The wave-function norm is equivalent to the Ising partition function. A Rokhsar-Kivelson type Hamiltonian is further derived by the stochastic matrix form[28]: $H^z = H_{\text{TC}} + \sum_j V_j$, with $V_j = \prod_{i \in \text{star}(j)} \left(\frac{1-h}{1+h} \right)^{\sigma_{i,j}^x}$. Note $V_j \rightarrow \infty$ when $h \rightarrow 1$, which is the reason why we require $h < 1$. By electric-magnetic duality, the confining phase transition at $\theta = 0$ can be solved as well, and the phase diagram is shown in Fig. 1b. However, away from the limits $\theta = 0, \pi/2$, it is much less understood. Especially, $\theta = \pi/4$ corresponds to the electric-magnetic self-dual path:

$$|\psi\rangle = \prod_{\langle i,j \rangle} \left(1 + h \frac{\sigma_{i,j}^z + \sigma_{i,j}^x}{\sqrt{2}} \right) |1\rangle. \quad (5)$$

The main result of this work is that, the self-dual toric code phase can undergo a quantum KT phase transition into a gapless Coulomb state, as shown in Fig. 1c.

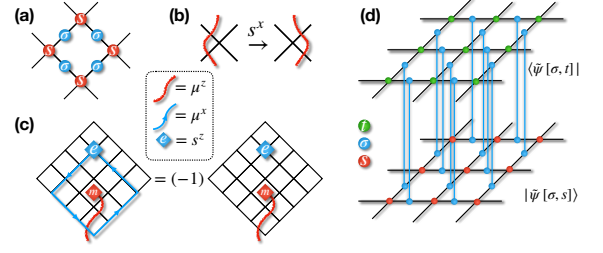


FIG. 2: (a) The entangled state between physical gauge spins labeled by blue dots on the links and auxiliary matter spins labeled by red dots on the vertices. (b) The local Z_2 gauge symmetry s^x deforms the magnetic flux tube generated by a sequence of μ^z . (c) The electric charge can be moved by μ^x , and it acquires π -phase across the magnetic flux tube. (d) The norm of the quantum wave-function is composed of double layers representing the ket and bra states, respectively. The physical spins are contracted, while the auxiliary spins from the ket and the bra layers are projected onto the product state $|+\rangle$ by the gauge constraint.

Mapping to the Ashkin-Teller model.— In his original paper, Kitaev introduced the Higgs matter spins to entangle the gauge spins so as to turn the toric code model into a gauge invariant theory[1]. Here we use a similar procedure to rewrite the deformed wave-function in the extended Hilbert space with a set of auxiliary Ising spins on each vertex restricted in the product state of s_j^x : $|+\rangle_s \equiv \prod_j |+\rangle_j$. In Fig. 2a, we show the deformed wave-function Eq.5 expressed as an entangled state of the physical "gauge" spins and auxiliary "matter" spins:

$$|\tilde{\psi}\rangle = \prod_{\langle i,j \rangle} \left(1 + h \frac{\sigma_{i,j}^z + \sigma_{i,j}^x}{\sqrt{2}} \right) P_s \frac{(1 + s_j^z s_j^z \sigma_{i,j}^z)}{2} |+\rangle_s |+\rangle_\sigma,$$

where $P_s = (1 + M_y)/\sqrt{2}$ projects onto the vacuum sector. Detailed derivation is given in Supplementary Material.

The physical subspace is subjected to the gauge constraint $s_j^x = 1$, and the auxiliary spin can be reduced by projection $|\psi\rangle = {}_s\langle + | \tilde{\psi} \rangle$. The local Z_2 gauge symmetry generated by s_j^x becomes more transparent when viewed from the dual disorder operator of s_j^z ,

$$\mu_{i,j}^x = s_i^z s_j^z, \quad s_j^x = \prod_{k \in \text{star}(j)} \mu_{j,k}^z. \quad (6)$$

In Fig. 2b, we show that an arbitrary string defect of disorder operator[29–31] $M_{(p,q)} \equiv \prod_{\langle i,j \rangle \in S(p,q)} \mu_{i,j}^z$ ending at plaquette p and q is free to fluctuate under the gauge symmetry. It can be identified as the magnetic flux tube, on whose end points live a pair of the magnetic flux excitations m_p and m_q on the plaquettes. Hence the dual Wilson line can be effectively implemented by a closed string of disorder creator: $M_y = \prod_{\langle i,j \rangle} \mu_{i,j}^z$. The electric charge is created by s_j^z , which can be moved by the action of $\mu_{i,j}^x$. Since $\mu^x \mu^z = -\mu^z \mu^x$, the electric charge acquires

a π phase whenever its trajectory crosses the magnetic flux tube (see Fig. 2c). In this way, m serves as a π -flux for e , and the semionic mutual statistics between e and m is thus verified. To conclude, the excitation of a pair of electric charges and magnetic fluxes can be written as

$$|e_i, e_j\rangle = {}_s\langle + | s_i^z s_j^z | \tilde{\psi} \rangle, |m_p, m_q\rangle = {}_s\langle + | M_{(p,q)} | \tilde{\psi} \rangle. \quad (7)$$

Consider the norm of the wave-function, which is viewed as a double-layer tensor-network shown schematically in Fig. 2d. The key observation is that if the physical spins are contracted out, the network evaluates the partition function of the classical isotropic AT model for the two layers of Ising auxiliary spins:

$$\langle \psi[\sigma, t] | \psi[\sigma, s] \rangle = \sum_{\{s, t\}} P_s P_t \prod_{\langle i, j \rangle} e^{-\epsilon_{i,j}} = Z_{\text{AT}}[s, t], \quad (8)$$

where

$$\begin{aligned} \epsilon_{i,j} &= -J(s_i s_j + t_i t_j) - J_4 s_i s_j t_i t_j - J_0, \\ J &= \frac{1}{4} \log \left(\frac{h^2 + \sqrt{2}h + 1}{h^2 - \sqrt{2}h + 1} \right), \quad J_4 = \frac{1}{4} \log \frac{1 + h^4}{2h^2}, \end{aligned} \quad (9)$$

and s_j and t_j are the quantum number of s_j^z and t_j^z . The factor $P_s P_t$ implements the dual Wilson line projectors on the ket and bra layers, equivalent to twisting the boundary condition. Notice that the self-duality condition of the AT model $e^{-2J_4} = \sinh(2J)$ is always satisfied, so that our self-dual quantum state Eq.5 is exactly mapped to the self-dual isotropic AT model[32]. As the anyon creating operators exactly correspond to the local spin operators or the domain wall flipping operators of the classical AT model, the classical phase transitions serve as the faithful detections for the topological phase transitions.

Next we briefly review the phase regime in the classical counterpart of our quantum state. When $h < h_c \equiv \sqrt{2} - 1$, $J_4 > J$ and the classical model sits in the partial order phase with $\langle s_j \rangle = \langle t_j \rangle = 0$ but $\langle s_j t_j \rangle \neq 0$, exactly corresponding to the topological order phase of the toric code model. However, for $h \geq h_c$, $J_4 \leq J$ and the classical model enters into the continuously varying critical phase with a fixed central charge 1, described by the conformal invariant Gaussian scalar field theory[32, 33]: $S = \frac{R^2}{8\pi} \int dz d\bar{z} \partial_z \phi \partial_{\bar{z}} \phi$. The field is compactified on a circle with the radius

$$R = 4 \sqrt{\frac{1}{\pi} \sin^{-1} \left(\frac{1}{2} \sqrt{1 + \frac{1 + h^4}{2h^2}} \right)}. \quad (10)$$

and orbifolded $\phi = -\phi$. Thus, the transition point $h = h_c$ has an enhanced symmetry S_4 , corresponding to the critical point of the $q = 4$ Potts model, i.e. the Z_2 orbifolding version of the KT critical point[34].

Anyon correlation functions.— With the classical phase diagram, we can switch back to the quantum wave-function and investigate the fate of anyons across the transition. With the electric-magnetic self-duality, the magnetic flux is supposed to follow the same behavior as the electric charge, so we focus on the electric charge. First, we measure the confinement by the diagonal correlators of a pair of separated electric charges: $\langle e_j, e_i | e_i, e_j \rangle$, a superposition of all the possibly deformed spatial Wilson loops pinned by two sites i and j . Alternatively, it can be simply viewed as the normalization constant of the charge excited state created from the ground state vacuum[15, 16]. By the quantum-classical correspondence, we thus establish that such a diagonal anyon correlation is equivalent to the correlation of polarization operator of the AT model, whose asymptotic behavior is exactly known from the scaling dimension[35]:

$$\begin{aligned} \langle e_j, e_i | e_i, e_j \rangle &= \langle s_j^z t_j^z s_i^z t_i^z \rangle_{Z_{\text{AT}}} \\ &\sim \begin{cases} C^2 (1 + O(e^{-|i-j|/\xi})) & h < h_c, \\ |i-j|^{-\frac{2}{R^2}} & h \geq h_c, \end{cases} \end{aligned}$$

where ξ is the correlation length in the toric code, and $\langle \cdot \rangle_{Z_{\text{AT}}}$ denotes the ensemble average of the classical model.

To measure the force-law between charges, a usual way is to place a pair of static test-charges separated in space and measure the free energy dependence of the distance, which can be calculated by the correlations of two Wilson lines stretching in the temporal direction of the lattice gauge theory[36]. Similarly, the diagonal anyon correlation function measures the probability amplitude of the existence of a pair of static charges, from which we might define a dimensionless "free energy": $\langle e_j, e_i | e_i, e_j \rangle \equiv e^{-F(|i-j|)}$. Then we have

$$F(|i-j|) \sim \begin{cases} O(e^{-|i-j|/\xi}) & h < h_c, \\ \frac{2}{R^2} \log|i-j| & h \geq h_c, \end{cases} \quad (11)$$

which shows the qualitative change of the spatial dependence of $F(|i-j|)$, the hallmark of the topological phase transition. In the deformed toric code phase with $h < h_c$, the result signifies a screened potential for the deconfined charges, characteristic of a plasma phase. However, for $h > h_c$, the electric charges are weakly confined by a logarithmic potential, characteristic of the 2D Coulomb state. The strength of the potential is determined by the anomalous dimension of the associated correlation function. The magnetic fluxes are likewise logarithmically confined, but the interaction between electric charge and magnetic flux involves an additional phase winding term, because they play the role of half vortex for each other.

Second, to consider the condensation, we measure only the pair condensation by virtue of the off-diagonal anyon correlator, which is defined by the overlap between the

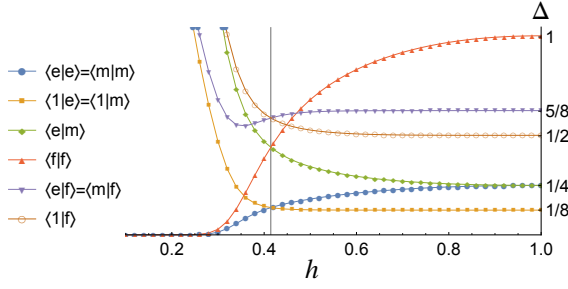


FIG. 3: Scaling dimensions numerically extracted from the eigenvalues of the transfer matrix for each anyon blocks, where we set $\Delta_{\langle 1|1 \rangle} = 0$. The velocity parameter is estimated as $v \approx 0.998$ and the circumference of the transfer matrix is chosen as $L_y = 10$. The vertical line near $h_c = \sqrt{2} - 1 \approx 0.414$ denotes the KT phase transition point.

ground state and the normalized state with charges pair:

$$\begin{aligned} \langle \psi | e_i, e_j \rangle / \| |e_i, e_j \rangle \| &= \langle s_i^z s_j^z \rangle_{Z_{AT}} / \sqrt{\langle s_i^z s_j^z t_i^z t_j^z \rangle_{Z_{AT}}} \\ &\sim \begin{cases} O(e^{-|i-j|/\xi}) & h < h_c, \\ |i-j|^{-(\frac{1}{4} - \frac{1}{R^2})} & h \geq h_c, \end{cases} \end{aligned}$$

where $\|\cdot\|$ denotes the state norm and the scaling dimension of s_j^z is known as $\Delta_s = 1/8$. There is also qualitative change to the condensation measurement. When $h < h_c$, the disorder of the classical Ising layers amounts to an exponential suppression of the tunneling between the quantum ground state and the charge excited state, and hence no condensation occurs. When $h > h_c$, the quasi-long-range order of the classical model leads to a power-law decay of the overlap between the ground state and charge excited pairs, indicative of a gapless condensate of bounded charge pairs.

One might ask what happens to the fermion excitations, which also are one of the anyon types in the toric code phase. One could likewise measure $\langle f_{j,q}, f_{i,p} | f_{i,p}, f_{j,q} \rangle$ for the confinement and $\langle \psi | f_{i,p}, f_{j,q} \rangle$ for the condensation. Due to the lack of the exact scaling dimension of the string defect, we can numerically extract the scaling dimensions of all the anyon correlations by diagonalizing the quantum transfer matrix. As there are four topological sectors in the ket and bra tensor layers, separately, we have 16 blocks of the transfer operator in total, and they are labeled by $\langle \alpha | \beta \rangle$ with $\alpha, \beta = 1, e, m, f$. The leading eigenvalue for each block can be parametrized as $\lambda_{\langle \alpha | \beta \rangle} = \lambda_{\langle 1 | 1 \rangle} e^{-\frac{2\pi v}{L_y} \Delta_{\langle \alpha | \beta \rangle}}$, where the velocity v is a non-universal constant that can be fitted by the exactly known result $\Delta_{\langle e | e \rangle} = \Delta_s = 1/8$ at the decoupling Ising point $h = 1$. When those fermionic correlations are expressed as

$$\begin{aligned} \langle f_{i,p}, f_{j,q} | f_{i,p}, f_{j,q} \rangle &\sim |i-j|^{-2\Delta_{\langle f | f \rangle}}, \\ \langle \psi | f_{i,p}, f_{j,q} \rangle &\sim |i-j|^{-2\Delta_{\langle 1 | f \rangle}}. \end{aligned} \quad (12)$$

we estimate $\Delta_{\langle f | f \rangle} \approx 4/R^2$ and $\Delta_{\langle 1 | f \rangle} \approx 1/2$ slightly

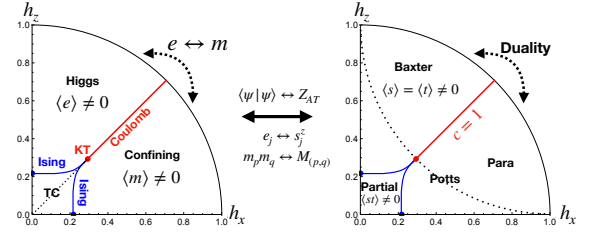


FIG. 4: The left panel shows the quantum phase diagram of the deformed toric code wave-function, which can be mapped in one-to-one correspondence to the phase diagram of the isotropic AT model on the right. The electric-magnetic duality in the quantum wave-function coincides with the Kramers-Wannier duality of the AT model, which transposes the phase diagram. $h_x \equiv h \cos \theta$, $h_z \equiv h \sin \theta$. The blue lines are located by quantum fidelity, see supplementary material.

away from the KT transition point, as shown in Fig. 3. Then these fermions are confined by a logarithmic potential, approximately four times that of the charges/fluxes. The full momentum resolved spectrum of the transfer operator is included in Supplementary Material.

Global phase diagram.— What is the instability of the phases in the absence of electric-magnetic self-duality? For the global phase diagram defined by Eq.4, it can be shown that the deformed toric code wave-function along any angle θ can be exactly mapped to the generalized isotropic AT model with

$$J = \frac{1}{4} \log \frac{1 + h^2 + 2h \sin \theta}{1 + h^2 - 2h \sin \theta}, \quad J_4 = \frac{1}{4} \log \frac{1 + h^4 + 2h^2 \cos 2\theta}{2h^2 (\cos 2\theta + 1)}.$$

So we can draw a complete topological-classical correspondence between the phase transitions of the deformed toric code wave-function and the AT model (Fig. 4). The Baxter phase in the AT model[37] has a long range order with $\langle s^z \rangle = \langle t^z \rangle = \langle s^z t^z \rangle \neq 0$, corresponding to the single electric charge condensation in the quantum state with $\langle e_i | \psi \rangle = \langle s_i^z \rangle / \sqrt{\langle s_i^z t_i^z \rangle} \neq 0$, i.e. the Higgs phase. The domain wall costs an energy linearly proportional to its length, signifying the confinement of magnetic fluxes. In the disorder paramagnetic phase of the AT model, $\langle s^z \rangle = \langle t^z \rangle = \langle s^z t^z \rangle = 0$ and the correlation function decays exponentially with a correlation length, and a linear confining potential is resulted $F(|i-j|) = -\log \langle e_j, e_i | e_i, e_j \rangle \sim |i-j|/\xi$ for the electric charges, corresponding to the confining phase.

The Coulomb state corresponds to the self-dual continuously varying criticality of the AT model, which further bifurcates at the critical point of the $q = 4$ Potts model into two 2D Ising transition lines accounting for the Higgs and confining transitions, respectively. When the self-duality is absent, the gapless Coulomb state falls immediately into the confining phase or Higgs phase. In the former phase, the magnetic flux condenses and develops a linearly confining potential for the electric charges, while in the latter phase the electric charges get decon-

finer and condensed. On the critical line, the electric charge is weakly confined and there emerges a $U(1)$ symmetry. In this sense, such a transition shares certain similarities with the deconfined quantum criticality[38]. It is expected that the effective theory comprises a non-compact $U(1)$ gauge field coupled to the massless bosonic charge, and the quantum KT critical point characterizes the charge-2e Higgs transition.

Conclusion and Outlook.- We have elucidated the topological phase transitions out of the toric code phase along the electric-magnetic self-duality. The novel topological phase transition is beyond the conventional Ginzburg-Landau paradigm, exhibiting the time-independent conformal symmetry[39] which usually occurs in the Rokhsar-Kivelson type models[40]. The obtained tensor-network wave functions can serve as a variational ansatz for the deformed model Hamiltonians. As the bond dimension of local tensors increases, the more

generic phases can be explored[27, 41]. We expect that the critical line of the Coulomb state becomes a first-order phase transition line, and the quantum KT transition could flow to its Lorentz invariant analog, namely, a 3D XY critical point characterizing the charge-2e Higgs transition between the Z_2 deconfined phase and the $U(1)$ confined phase[2, 42]. Therefore, our study provides a useful method to tackle the global phase diagram of the generic toric code Hamiltonian[6]. Meanwhile, it can also be generalized to investigate the Z_n gauge deconfined phases[43, 44] and the nonabelian phase[45, 46].

Acknowledgment.- The authors would like to thank Wen-Tao Xu and Shao-Kai Jian for their stimulating discussions and acknowledge the support by the National Key Research and Development Program of MOST of China (2017YFA0302902)).

SUPPLEMENTARY MATERIAL FOR "GAPLESS COULOMB PHASE EMERGED FROM A SELF-DUAL TOPOLOGICAL TENSOR-NETWORK STATE"

Introduction of the auxiliary matter spins

In the toric code model, the electric charge or magnetic flux is conserved modulo 2 even under perturbations as long as the phase transition does not occur. This implies a hidden $Z_2 \times Z_2$ symmetry. To explain the origin of such a symmetry, Kitaev extended the Hilbert space and introduced the Higgs matter field on vertex/plaquette, which is yet subjected to a local constraint[1]. The artificial constraint actually is lifted to a Z_2 gauge symmetry and has rather physical meaning. Especially, after a unitary transform for the extended Hilbert space, the gauge symmetry is in a more familiar look as in the conventional lattice gauge theory[2]. In dealing with the wave-function, one could do a similar procedure. For the sake of clearness we show how to introduce the matter spin to entangle with the physical gauge spin in the simplest plain ground state wave-function without deformation or global projection: $|\psi_0\rangle = \prod_j \frac{1+A_j}{\sqrt{2}} |\uparrow\rangle_\sigma$.

First we extend the Hilbert space and introduce the auxiliary matter spin in the x polarized state $|+\rangle_s$ on the vertex:

$$|\psi_0\rangle \rightarrow |\tilde{\psi}_0\rangle \equiv P_G |\psi_0\rangle \otimes |+\rangle_s, \quad (13)$$

where the projector $P_G = \prod_j \frac{1+s_j^x}{2}$ is to enforce the local gauge constraint $s_j^x = 1$ in the extended state. This might seem trivial at first glance, but if the gauge constraint is strictly enforced, within the gauge invariant physical space

one can derive that

$$\begin{aligned}
|\tilde{\psi}_0\rangle &= P_G \prod_j \frac{1 + A_j}{\sqrt{2}} |+\rangle_s |\uparrow\rangle_\sigma \\
&= P_G \prod_j \frac{1 + s_j^x A_j}{\sqrt{2}} |+\rangle_s |\uparrow\rangle_\sigma \\
&= P_G \prod_j (1 + s_j^x A_j) \frac{1 + s_j^x}{2} |\uparrow\rangle_s |\uparrow\rangle_\sigma \\
&= P_G \prod_j (1 + s_j^x A_j) |\uparrow\rangle_s |\uparrow\rangle_\sigma \\
&= P_G \sum_{\{s,\sigma\}} \prod_{\langle i,j \rangle} \frac{1 + s_j \sigma_{i,j} s_i}{2} |s\rangle |\sigma\rangle \\
&= P_G \prod_{\langle i,j \rangle} \frac{1 + s_j^z \sigma_{i,j}^z s_i^z}{2} |+\rangle_s |+\rangle_\sigma.
\end{aligned} \tag{14}$$

We can see that even without a unitary transform to change the looking of the gauge symmetry, one can rewrite the wave-function into an entangled state between the physical gauge spins and auxiliary spins, by virtue of the gauge constraint. To reduce the redundant matter spins in the wave-function, one can simply project the extended state onto the gauge invariant subspace:

$$\begin{aligned}
|\psi_0\rangle &= {}_s\langle + | \tilde{\psi}_0 \rangle \\
&= {}_s\langle + | \prod_{\langle i,j \rangle} \frac{1 + s_j^z \sigma_{i,j}^z s_i^z}{2} |+\rangle_s |+\rangle_\sigma \\
&= \sum_{\{s\}} \prod_{\langle i,j \rangle} \frac{1 + s_j s_i \sigma_{i,j}^z}{2} |+\rangle_\sigma.
\end{aligned} \tag{15}$$

The introduction of auxiliary matter spins is robust against the physical deformation, and therefore we have the extended deformed wave-function:

$$|\tilde{\psi}(h, \theta)\rangle = P_G \prod_{\langle i,j \rangle} (1 + h (\sigma_{i,j}^x \cos\theta + \sigma_{i,j}^z \sin\theta)) \frac{1 + M_y}{\sqrt{2}} \frac{1 + s_j^z \sigma_{i,j}^z s_i^z}{2} |+\rangle_s |+\rangle_\sigma, \tag{16}$$

whose projection onto the gauge invariant subspace reduces the auxiliary degrees of freedom:

$$|\psi(h, \theta)\rangle = {}_s\langle + | \tilde{\psi}(h, \theta) \rangle. \tag{17}$$

A brief remark: one can see that actually in this way the wave-function turns to the tensor-network formalism, where the quantum numbers of the auxiliary matter spins play the role of the virtual bond dummy variables. That is the reason why the symmetry breaking pattern in the virtual space of the transfer matrix[14, 15] can correspond to the Higgs transition, where the gauge symmetry is spontaneously broken due to the matter field.

Derivation of the Boltzman weight

When restricted to the given wave-function, the auxiliary spin s_j plays the role of a dummy variable in generating the wave-function $|\psi\rangle$. The auxiliary spin that generates $\langle\psi|$, on the other hand, has nothing to do with and should be independent from the s_j , which we might label as t_j . Therefore, we have two layers of Ising spins in representing a generic correlation function out of the ground state, which is consistent with the tensor-network formalism. By contracting the physical degree of freedom in the wave-function,

$$|\psi(h, \theta)\rangle = \sum_{\{s\}, \{\sigma\}} P_s \prod_{\langle i,j \rangle} \left((1 + h \sin\theta \sigma_{i,j}) \frac{1 + s_i s_j \sigma_{i,j}}{2} + h \cos\theta \frac{1 - s_i s_j \sigma_{i,j}}{2} \right) |\sigma_{i,j}\rangle, \tag{18}$$

where σ is the quantum number of σ^z , one can derive the norm as the partition function of $\{s, t\}$:

$$\langle \psi | \psi \rangle = \sum_{\{s, t\}} P_s P_t \prod_{\langle i, j \rangle} \omega_{i, j}, \quad (19)$$

where the local "Boltzman weight" is

$$\omega_{i, j} = \left((1 + h \sin \theta s_i s_j)^2 + h^2 \cos^2 \theta \right) \frac{1 + s_i s_j \sigma_i \sigma_j}{2} + 2h \cos \theta \frac{1 - s_i s_j \sigma_i \sigma_j}{2} \equiv e^{-\epsilon_{i, j}}. \quad (20)$$

As there are two independent parameters (h, θ) , taking the global normalization constant into account, one has three parameters. Therefore, three energy levels for the 16 local configurations consist of 4 spins (s_i, s_j, t_i, t_j) , which can be parametrized by three parameters in the energy form $\epsilon_{i, j} = -J(s_i s_j + t_i t_j) - J_4 s_i s_j t_i t_j - J_0$. The 2-spin, 4-spin interactions and the constant terms are given as

$$\begin{aligned} J &= \frac{1}{4} \log \frac{1 + h^2 + 2h \sin \theta}{1 + h^2 - 2h \sin \theta}, \\ J_4 &= \frac{1}{4} \log \frac{1 + h^4 + 2h^2 \cos 2\theta}{2h^2 (\cos 2\theta + 1)}, \\ J_0 &= \frac{1}{4} \log ((1 + h^4 + 2h^2 \cos 2\theta) 2h^2 (\cos 2\theta + 1)). \end{aligned} \quad (21)$$

This is nothing but the classical isotropic Ashkin-Teller(AT) model, where two layers of Ising model are coupled by a four-spin interaction, as one of the natural extension lists of the well-known Ising model. It has been shown to be mapped to the staggered eight vertex model[37]. Especially, along the self-dual line with $e^{-2J_4} = \sinh(2J)$, it can be mapped to a line in the phase diagram of homogeneous eight vertex model, as well as dually mapped to the six vertex model, where there is a continuously varying $U(1)$ critical line separated from the disorder phase by the Kosterlitz-Thouless transition. Therefore, the AT model is one of the central models in the statistical mechanics whose criticality has been exactly solved. Notice that despite their similarities, distinct from the eight vertex model, the AT model has an exceptional partial order phase, whose phase boundary is the Ising transition lines bifurcated from the $q = 4$ Potts critical point. In our parametrization, the duality of the AT model is as simple as a flipping of the $h_x \leftrightarrow h_z$ or $\theta \leftrightarrow \pi/2 - \theta$. And the self-dual line lies on the $\theta = \pi/4$.

The correspondences of local operators

To extract the local operator correspondence between the quantum physical space and the classical auxiliary space, one has to insert the physical operator onto the physical level and contract out the physical spin, leaving a factor represented by the auxiliary spin $\omega'[s, t; \sigma^\alpha]$, where $\alpha = 0, x, y, z$. Then by subtracting the Boltzmann weight, one arrives at the corresponding classical operator $\tilde{\sigma}^\alpha \equiv \omega'[s, t; \sigma^\alpha] / \omega[s, t]$, such that

$$\langle \psi | \sigma_{i, j}^\alpha \sigma_{k, l}^\beta \cdots | \psi \rangle = \langle \tilde{\sigma}_{i, j}^\alpha \tilde{\sigma}_{k, l}^\beta \cdots \rangle_{\text{ZAT}}. \quad (22)$$

This procedure could be performed generically, but here we only show the result along the self-dual line:

$$\begin{aligned} \tilde{\sigma}_{i, j}^z &= \frac{1}{2\sqrt{2}(1 + h^4)} \left(h(1 + h^2)^2 + \sqrt{2}(1 - h^2)(s_i s_j + t_i t_j) - h(1 - h^2)^2 s_i s_j t_i t_j \right), \\ \tilde{\sigma}_{i, j}^x &= \frac{1}{2\sqrt{2}(1 + h^4)} \left(\frac{1}{h}(1 + h^2)^2 - \sqrt{2}h^2(1 - h^2)(s_i s_j + t_i t_j) - \frac{1}{h}(1 - h^2)^2 s_i s_j t_i t_j \right), \\ i\tilde{\sigma}_{i, j}^y &= \frac{1 - h^2}{2\sqrt{2}h} (s_i s_j - t_i t_j). \end{aligned} \quad (23)$$

If one is careful enough to investigate into the expression above, one could be alert to find that at some limit points the mapping between some of the local operators could break down. For example, the limit $h = 1$ has $\tilde{\sigma}^z = \tilde{\sigma}^x = 1/\sqrt{2}$, $\tilde{\sigma}^y = 0$, so that the local operators in the quantum state is blinded to any singularity behaviour at the classical counterpart, which is in the decoupled Ising critical point (Ising)². Indeed, at the limit $h = 1$ the quantum state is just a trivial product state, although the classical model is in the decoupled Ising critical point.

From another angle it is reasonable for the mapping to break down at the particular decoupled Ising point, because the ket and bra layer are never supposed to be completely "decoupled". In this sense, $h = 1$ is a very special limit point that cannot represent the physics in $h < 1$, justifying our choosing the phase regime $h \in [0, 1)$. Another hint that justifies excluding the $h = 1$ limit is some coupling constants in the RK Hamiltonian blow up towards the limit $h \rightarrow 1$.

Quantum fidelity for the phase transitions

With the exact ground state in hand, we could numerically probe the phase diagram by using quantum fidelity straightforwardly[21, 47]. We measure the quantum fidelity F_h when h is perturbed with θ being fixed, and the quantum fidelity F_θ when h is fixed but θ is varied:

$$\begin{aligned} F_h &\equiv \langle \psi(h, \theta) | \psi(h + \delta h, \theta) \rangle = e^{-g_h \delta h^2 N}, \\ F_\theta &\equiv \langle \psi(h, \theta) | \psi(h, \theta + \delta \theta) \rangle = e^{-g_\theta h^2 \delta \theta^2 N}, \end{aligned} \quad (24)$$

from which we can extract the quantum fidelity metric along the radial (azimuthal) direction $g_h(\theta)$ with N being the total number of lattice sites. The numerical calculation is shown in Fig. 5. Notice that, without the support of the analytical results, it would be tough to pinpoint the accurate position of the critical point of the 4-state Potts model by merely numerical calculation, which suffers from the logarithmic finite size effect, characteristic of KT transition[48].

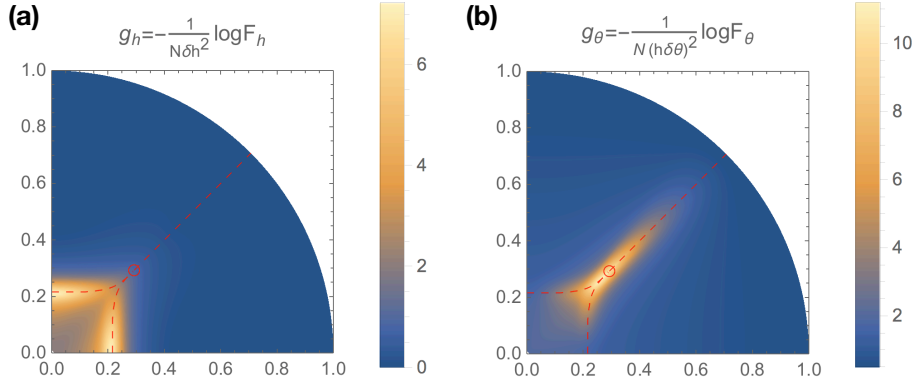


FIG. 5: Quantum fidelity metric. (a) θ is fixed, h is varied. (b) θ is varied, h is fixed. The red dashed line marks the location of metric peak, i.e. the phase transition lines. The red open circle denotes the exact location of the Potts point to guide the vision. In the calculation of wave-function overlap, we take a $(L_y = 6) \times (L_x = 100)$ tensor-network, where the local tensors are located on half of the plaquette centers.

Full spectrum of the transfer matrix at the critical points

We calculate a complete spectrum of the transfer matrix at the phase transition point $h = \sqrt{2} - 1$, resolved by momentum in Fig. 6a. The transfer matrix has 10 independent blocks corresponding to the four anyon sectors in bra and the four anyon sectors in ket. The lowest excited levels corresponding to the anyon block $\langle e|e \rangle$ and $\langle 1|e \rangle$ have exact scaling dimension $1/8$ as expected analytically, and the corresponding conformal spins (rescaled momentum $kL_y/2\pi$) are 0. The lowest level in the block $\langle f|f \rangle$ is close to $(0, 1/2)$, parametrized by the Gaussian theory $\Delta = 4/R^2$, and the lowest level in block $\langle f|1 \rangle$ is close to $(1/2, 1/2)$. For comparison we also give the spectrum at the Ising decoupled limit $h = 1$ (Fig. 6b). Although the limit point $h = 1$ is excluded from our phase diagram, by comparing the spectrum between the transition point $h = \sqrt{2} - 1$ and that of the $h = 1$ point, one can get a glimpse of the evolution of the spectrum along increasing h . Except some levels due to the Z_2 orbifolding such as $\Delta = 1/8$, most of the primary levels can be rewritten in the Gaussian language labeled by the spin wave index n of operator $e^{in\phi}$ and vorticity index p of the scalar field: (n, p) [49]. The corresponding scaling dimension and conformal spin are parametrized by the radius

$$\Delta = \frac{n^2}{R^2} + \frac{p^2 R^2}{4}, \quad s = np. \quad (25)$$

For the Potts point, $R = 2\sqrt{2}$, and $R = 2$ for the decoupled Ising point. Note that we avoid the more common notation with e and m to denote the spin wave index and vortex index, so as to avoid confusion between the charge and vortex in the language of scalar field theory and that of the toric code.

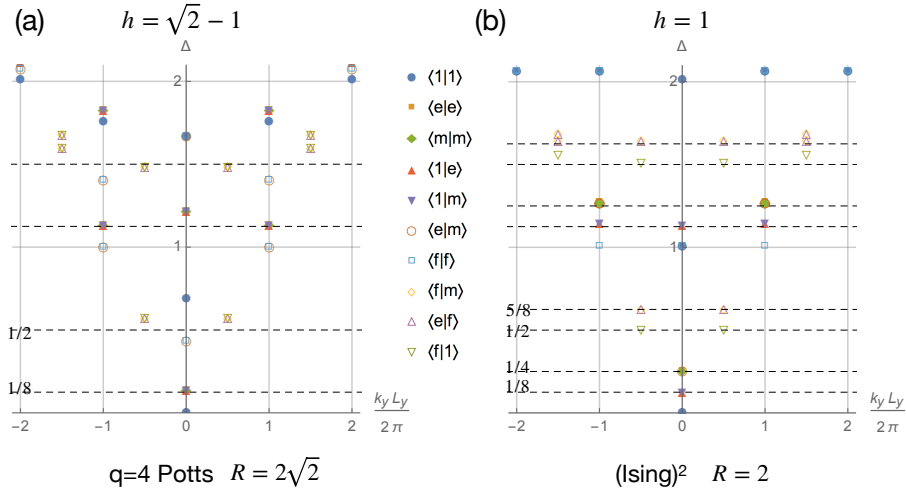


FIG. 6: (a) Exact diagonalization for the transfer matrix at the transition point $h = \sqrt{2} - 1, \theta = \pi/4$, resolved by momentum along the y direction. The eigenvalue $\lambda_{\langle \alpha|\beta \rangle} = \lambda_{\langle 1|1 \rangle} e^{-\frac{2\pi v}{L_y} \Delta_{\langle \alpha|\beta \rangle}}$. $v \approx 1.028$ and $L_y = 10$. The figure shows the corresponding scaling dimension Δ and scaled momentum for the levels in each anyon sectors. The dashed line marks the position of particular scaling dimension $\Delta = 1/8, 1/2$ and their descendants. In this numerical calculation the finite size effect is very strong. (b) Exact diagonalization for the transfer matrix at the Ising decoupled limit $h = 1, \theta = \pi/4$, resolved by momentum along the y direction. $v \approx 0.998$ and $L_y = 10$. The dashed line marks the position of particular scaling dimension $\Delta = 1/8, 1/4, 1/2, 5/8$ and their descendants.

-
- [1] A. Kitaev, Annals of Physics **303**, 2 (2003), ISSN 0003-4916, URL <http://www.sciencedirect.com/science/article/pii/S0003491602000180>.
- [2] E. Fradkin and S. H. Shenker, Phys. Rev. D **19**, 3682 (1979), URL <https://link.aps.org/doi/10.1103/PhysRevD.19.3682>.
- [3] G. A. Jongeward, J. D. Stack, and C. Jayaprakash, Phys. Rev. D **21**, 3360 (1980), URL <https://link.aps.org/doi/10.1103/PhysRevD.21.3360>.
- [4] S. Trebst, P. Werner, M. Troyer, K. Shtengel, and C. Nayak, Phys. Rev. Lett. **98**, 070602 (2007), URL <https://link.aps.org/doi/10.1103/PhysRevLett.98.070602>.
- [5] J. Vidal, S. Dusuel, and K. P. Schmidt, Phys. Rev. B **79**, 033109 (2009), URL <https://link.aps.org/doi/10.1103/PhysRevB.79.033109>.
- [6] I. S. Tupitsyn, A. Kitaev, N. V. Prokof'ev, and P. C. E. Stamp, Phys. Rev. B **82**, 085114 (2010), URL <https://link.aps.org/doi/10.1103/PhysRevB.82.085114>.
- [7] F. Wu, Y. Deng, and N. Prokof'ev, Phys. Rev. B **85**, 195104 (2012), URL <https://link.aps.org/doi/10.1103/PhysRevB.85.195104>.
- [8] S. Dusuel, M. Kamfor, R. Orús, K. P. Schmidt, and J. Vidal, Phys. Rev. Lett. **106**, 107203 (2011), URL <https://link.aps.org/doi/10.1103/PhysRevLett.106.107203>.
- [9] F. A. Bais and J. K. Slingerland, Phys. Rev. B **79**, 045316 (2009), URL <https://link.aps.org/doi/10.1103/PhysRevB.79.045316>.
- [10] X. Chen, B. Zeng, Z.-C. Gu, I. L. Chuang, and X.-G. Wen, Phys. Rev. B **82**, 165119 (2010), URL <https://link.aps.org/doi/10.1103/PhysRevB.82.165119>.
- [11] N. Schuch, I. Cirac, and D. Prez-Garcia, Annals of Physics **325**, 2153 (2010), ISSN 0003-4916, URL <http://www.sciencedirect.com/science/article/pii/S0003491610000990>.
- [12] N. Bultinck, M. Marin, D. Williamson, M. ahinolu, J. Haegeman, and F. Verstraete, Annals of Physics **378**, 183 (2017), ISSN 0003-4916, URL <http://www.sciencedirect.com/science/article/pii/S0003491617300040>.
- [13] S. K. Shukla, M. B. Şahinoğlu, F. Pollmann, and X. Chen, Phys. Rev. B **98**, 125112 (2018), URL <https://link.aps.org/doi/10.1103/PhysRevB.98.125112>.
- [14] N. Schuch, D. Poilblanc, J. I. Cirac, and D. Pérez-García, Phys. Rev. Lett. **111**, 090501 (2013), URL <https://link.aps.org/doi/10.1103/PhysRevLett.111.090501>.
- [15] J. Haegeman, V. Zauner, N. Schuch, and F. Verstraete, NATURE COMMUNICATIONS **6**, 8 (2015), ISSN 2041-1723, URL <http://dx.doi.org/10.1038/ncomms9284>.
- [16] K. Duivenvoorden, M. Iqbal, J. Haegeman, F. Verstraete, and N. Schuch, Phys. Rev. B **95**, 235119 (2017), URL <https://link.aps.org/doi/10.1103/PhysRevB.95.235119>.
- [17] W.-T. Xu and G.-M. Zhang, Phys. Rev. B **98**, 165115 (2018), URL <https://link.aps.org/doi/10.1103/PhysRevB.98.165115>.
- [18] C. Castelnovo and C. Chamon, Phys. Rev. B **77**,

- 054433 (2008), URL <https://link.aps.org/doi/10.1103/PhysRevB.77.054433>.
- [19] C. Castelnovo, S. Trebst, and M. Troyer, *Topological Order and Quantum Criticality* (2010), pp. 169–192.
- [20] X.-Y. Feng, G.-M. Zhang, and T. Xiang, Phys. Rev. Lett. **98**, 087204 (2007), URL <https://link.aps.org/doi/10.1103/PhysRevLett.98.087204>.
- [21] J. Haegeman, K. Van Acoleyen, N. Schuch, J. I. Cirac, and F. Verstraete, Phys. Rev. X **5**, 011024 (2015), URL <https://link.aps.org/doi/10.1103/PhysRevX.5.011024>.
- [22] L. Vanderstraeten, M. Mariën, J. Haegeman, N. Schuch, J. Vidal, and F. Verstraete, Phys. Rev. Lett. **119**, 070401 (2017), URL <https://link.aps.org/doi/10.1103/PhysRevLett.119.070401>.
- [23] M. Iqbal, K. Duivenvoorden, and N. Schuch, Phys. Rev. B **97**, 195124 (2018), URL <https://link.aps.org/doi/10.1103/PhysRevB.97.195124>.
- [24] R. B. Laughlin, Phys. Rev. Lett. **50**, 1395 (1983), URL <https://link.aps.org/doi/10.1103/PhysRevLett.50.1395>.
- [25] J. M. Kosterlitz and D. J. Thouless, Journal of Physics C: Solid State Physics **6**, 1181 (1973), URL <https://doi.org/10.1088>.
- [26] M. A. Levin and X.-G. Wen, Phys. Rev. B **71**, 045110 (2005), URL <https://link.aps.org/doi/10.1103/PhysRevB.71.045110>.
- [27] S. V. Isakov, P. Fendley, A. W. W. Ludwig, S. Trebst, and M. Troyer, Phys. Rev. B **83**, 125114 (2011), URL <https://link.aps.org/doi/10.1103/PhysRevB.83.125114>.
- [28] C. L. Henley, Journal of Physics: Condensed Matter **16**, S891 (2004), URL <http://stacks.iop.org/0953-8984/16/i=11/a=045>.
- [29] M. Hauru, G. Evenbly, W. W. Ho, D. Gaiotto, and G. Vidal, Phys. Rev. B **94**, 115125 (2016), URL <https://link.aps.org/doi/10.1103/PhysRevB.94.115125>.
- [30] D. Aasen, R. S. K. Mong, and P. Fendley, Journal of Physics A: Mathematical and Theoretical **49**, 354001 (2016), URL <https://doi.org/10.1088/2F1751-8113/2F49/2F35/2F354001>.
- [31] J. C. Bridgeman, S. D. Bartlett, and A. C. Doherty, Phys. Rev. B **96**, 245122 (2017), URL <https://link.aps.org/doi/10.1103/PhysRevB.96.245122>.
- [32] H. Saleur, Journal of Statistical Physics **50**, 475 (1988), ISSN 1572-9613, URL <https://doi.org/10.1007/BF01026488>.
- [33] H. Saleur, Journal of Physics A: Mathematical and General **20**, L1127 (1987), URL <https://doi.org/10.1088>.
- [34] R. Dijkgraaf, E. Verlinde, and H. Verlinde, Communications in Mathematical Physics **115**, 649 (1988), ISSN 1432-0916, URL <https://doi.org/10.1007/BF01224132>.
- [35] L. P. Kadanoff and A. C. Brown, Annals of Physics **121**, 318 (1979), ISSN 0003-4916, URL <http://www.sciencedirect.com/science/article/pii/0003491679901003>.
- [36] B. Svetitsky and L. G. Yaffe, Nuclear Physics B **210**, 423 (1982), ISSN 0550-3213, URL <http://www.sciencedirect.com/science/article/pii/0550321382901729>.
- [37] R. J. Baxter, *Exactly solved models in statistical mechanics* (Academic Press, London, Inc, 1982).
- [38] T. Senthil, A. Vishwanath, L. Balents, S. Sachdev, and M. P. A. Fisher, Science **303**, 1490 (2004), ISSN 0036-8075, URL <http://science.sciencemag.org/content/303/5663/1490>.
- [39] E. Ardonne, P. Fendley, and E. Fradkin, Annals of Physics **310**, 493 (2004), ISSN 00034916, URL <http://linkinghub.elsevier.com/retrieve/pii/S0003491604000247>.
- [40] D. S. Rokhsar and S. A. Kivelson, Phys. Rev. Lett. **61**, 2376 (1988), URL <https://link.aps.org/doi/10.1103/PhysRevLett.61.2376>.
- [41] L. Tagliacozzo, A. Celi, and M. Lewenstein, Phys. Rev. X **4**, 041024 (2014), URL <https://link.aps.org/doi/10.1103/PhysRevX.4.041024>.
- [42] T. Hansson, V. Oganesyan, and S. Sondhi, Annals of Physics **313**, 497 (2004), ISSN 0003-4916, URL <http://www.sciencedirect.com/science/article/pii/S0003491604001046>.
- [43] Z.-C. Gu, M. Levin, B. Swingle, and X.-G. Wen, Phys. Rev. B **79**, 085118 (2009), URL <https://link.aps.org/doi/10.1103/PhysRevB.79.085118>.
- [44] O. Buerschaper, M. Aguado, and G. Vidal, Phys. Rev. B **79**, 085119 (2009), URL <https://link.aps.org/doi/10.1103/PhysRevB.79.085119>.
- [45] A. Kitaev, Annals of Physics **321**, 2 (2006), ISSN 0003-4916, URL <http://www.sciencedirect.com/science/article/pii/S0003491605002381>.
- [46] H.-Y. Lee, R. Kaneko, T. Okubo, and N. Kawashima, arXiv e-prints (2019), 1901.05786.
- [47] P. Zanardi, P. Giorda, and M. Cozzini, Phys. Rev. Lett. **99**, 100603 (2007), URL <https://link.aps.org/doi/10.1103/PhysRevLett.99.100603>.
- [48] G. Sun, A. K. Kolezhuk, and T. Vekua, Phys. Rev. B **91**, 014418 (2015), URL <https://link.aps.org/doi/10.1103/PhysRevB.91.014418>.
- [49] F. C. Alcaraz, M. N. Barber, and M. T. Batchelor, Annals of Physics **182**, 280 (1988).